INDONESIAN JOURNAL ON GEOSCIENCE
Geological Agency
Ministry of Energy and Mineral Resources

Journal homepage: http://ijog.geologi.esdm.go.id
ISSN 2355-9314, e-ISSN 2355-9306

Structural and Karst Studies Using 3D Digital Outcrop Model: A Case Study in Gunung Keriang, Kedah, Peninsular Malaysia

Tan Yan Eng[1], Choong Chee Meng[2], Muhammad Amzar Bin Aznan[2], Amirruddin Bin Rosni[3], Muhammad Aslam MD Yusof[1], Muhammad Azfar Bin Mohamed[4], and Siti Sarah Binti A.B. Rahman[2]

[1]Petroleum Engineering Department, Universiti Teknologi PETRONAS, Malaysia
[2]Digital Geoscience Global Sdn Bhd (DGeG), Malaysia
[3]Malaysia Rock Products Sdn Bhd, Malaysia
[4]Centre for Advanced and Professional Education (CAPE), Universiti Teknologi PETRONAS, Malaysia

Corresponding author: tanyaneng@gmail.com
Manuscript received: November 24, 2023; revised: July, 25, 2024;
approved: August, 23, 2024; available online: October, 29, 2024

Abstract - A digital outcrop model (DOM) of the Permo-Triassic limestone of Gunung Keriang, Kedah, was constructed for structural analysis and karst study. Structural analysis of beddings and fractures within the DOM revealed that the limestone beds are characterized by gently inclined planes with NE−SW and NW−SE strikes, forming an upright N−S trending synclinal fold, and being cross-cut by four steeply-dipping fracture sets (NE−SW, NW−SE, N−S, and E−W). The synthesis of these fracture sets indicates that the NW−SE and NE−SW fractures form a conjugate pattern suggestive of E−W shortening, which aligns with the observed N−S fold. Karst development, including elongated sinkholes and cave paths oriented in the NE−SW direction, correlates with the fracture patterns, highlighting the NE−SW fracture network significant role in karst formation. The integrated data supports the hypothesis that these fracture patterns are major factors in the dissolution and development of karst features in the region.

Keywords: digital outcrop model (DOM), Gunung Keriang, fracture, limestone, photogrammetry

How to cite this article:
Tan, Y.E., Choong, C.M., Aznan, M.A., Rosni, A.B., Yusof, M.A.M.D., Mohamed, M.A.B., and Rahman, S.S.B.A.B., 2024. Structural and Karst Studies Using 3D Digital Outcrop Model: A Case Study in Gunung Keriang, Kedah, Peninsular Malaysia. *Indonesian Journal on Geoscience*, 11 (3), p.325-338. DOI: 10.17014/ijog.11.3.325-338

Introduction

The application of digital outcrop models (DOMs) for geoscience studies has become increasingly popular in the 21st century. Drone-based photogrammetry surveying is one of the most common techniques adopted for a highly detailed DOM construction. This technique allows for high-quality and high-count topographic photographs that fully represent the structure of an outcrop with a modest cost and simple survey planning. The advancements in DOM processing, visualization, and interpretation technologies have continuously expanded the use of DOM in geosciences.

Traditional geological mapping techniques often encounter challenges in tropical regions like Malaysia, where dense vegetation and challenging topography make rock outcrops and karst formations difficult to access. These conditions hinder the collection of sufficient structural data. This study addresses these challenges by introducing a robust digital geological data collection workflow designed specifically for structural and karst studies. The primary aim of this study is to demonstrate the application of DOMs for structural analysis in challenging environments. It evaluates how DOMs can be effectively utilized to conduct a detailed structural analysis in areas where traditional mapping methods are limited by accessibility issues. Additionally, the study aims to show how leveraging DOMs can enhance fracture analysis and structural understanding, providing a detailed geological information, even from inaccessible outcrops.

In NW Peninsular Malaysia, an isolated limestone hill, Gunung Keriang, located in Kedah state (Figure 1), offers the opportunity to demonstrate the digital structural analysis workflow. Field observations indicate that the limestones are bedded and fractured. They are typically concealed by thick vegetation, and the exposed rocks are usually located at the upper sections of steep cliffs (Figure 1).

Geological Setting

The Western Belt of Peninsular Malaysia is part of the Sibumasu Block, which originated from the NW Australian Gondwana margin during Late Early Permian (Metcalfe, 2011). The deposition of tropical limestone took place during Permo-Triassic when the Sibumasu Block drifted north to warmer latitudes, and eventually led to the collision with Indochina, resulting in faults and folds throughout the region. Currently, the limestone outcrops in the NW Peninsular Malaysia region forms a series of steep N-S trending continuous mountain ranges or isolated karstic hills in many

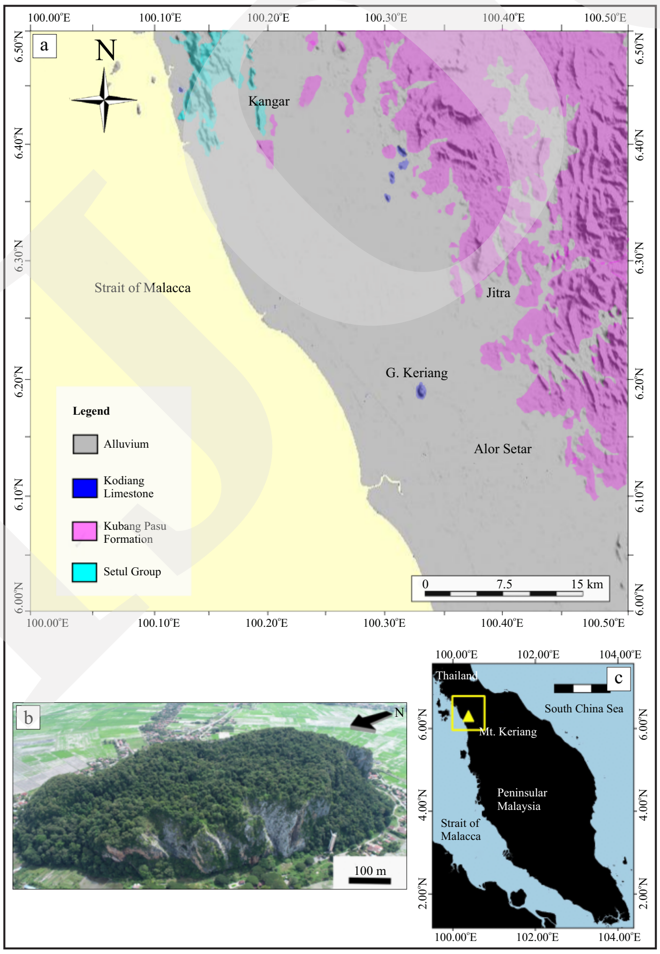

Figure 1. Gunung Keriang is in Kedah, located in the northwestern part of Peninsular Malaysia. (a) Geological map of north Kedah and Perlis. (b) Aerial photograph of Gunung Keriang outcrop. The hill has an area of roughly 0.6 km², and its peak stands at about 220 m. (c) Location of Gunung Keriang outcrop.

parts of Perlis and northern Kedah (Meor, 2013). Meanwhile, the structural trend in this region is generally NE-striking with continuous deposition during the Paleozoic (Foo, 1983). Gunung Keriang forms part of the N-S limestone mountain range, and is made up of the Permo-Triassic Chuping Formation. The Chuping Limestone mainly comprises massive limestone with fossilized well-bedded limestone at the base (Gobbett and Hutchison, 1973). The discovery of several fossils within the Chuping Formation supports an Early Permian to Late Triassic age (Kobayashi and Tamura, 1968), equivalent to the Kodiang Formation. Metcalfe (1981) (Figure 2) classified the limestone strata of Gunung Keriang into six lithology units: massive limestone, bedded limestone, bedded dolomitic limestone, slumped (possibly) bedded limestone, and chert. Late Wolfcampian (Early Permian) and Smithian (Early Triassic) conodonts were discovered in the massive dolomitic limestone and slumped (?) bedded limestone. The absence of the Middle and Late Permian strata is interpreted to be a major break in the sequence at the Permian-Triassic boundary (Metcalfe, 1981). Gunung Keriang comprises well-bedded limestone that forms a gentle fold trending N-S. Three major fracture sets were identified in Gunung Keriang, striking in the NW-SE, NE-SW, and N-S directions (Aznan *et al.*, 2024).

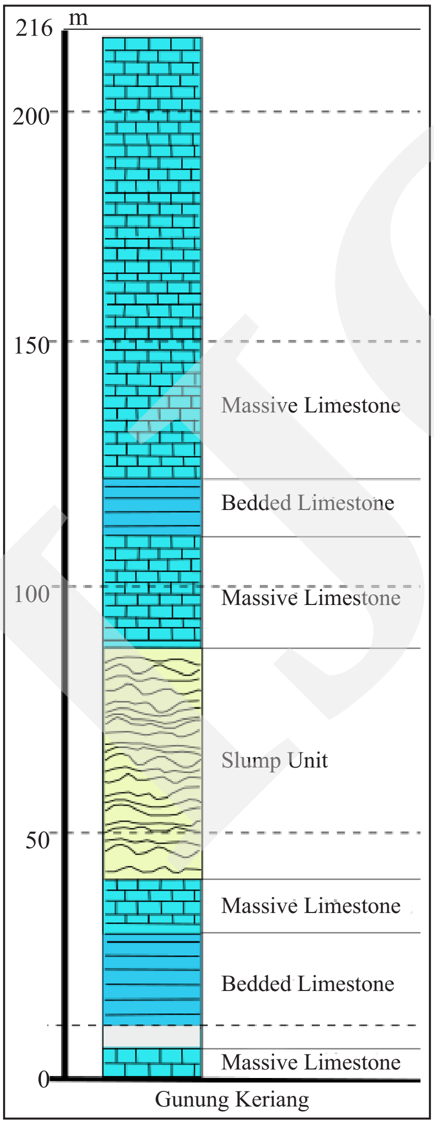

Figure 2. Stratigraphic column of Gunung Keriang (modified after Metcalfe, 1981).

Methods

The study was divided into three stages: (1) Data acquisition, (2) Digital outcrop model (DOM) building, and (3) Interpretation and analysis using DOM. The main workflow for this study is summarized in Figure 3.

Data Acquisition

The aerial photographs were acquired in 2022 to obtain high-resolution digital photographs of the outcrop. A DJI Phantom 4 Pro drone camera (model FC6310) with a 1-inch CMOS sensor was used to shoot 20MP resolution photos. The aircraft flew back and forth in parallel lines to cover the full extent of the outcrop at an altitude of 92 m to 511 m (Figure 4a). The aircraft was equipped with a positioning algorithm using signals from GPS/GLONASS to precisely geo-reference the images taken. Each digital photograph has 5472 x 3078 pixels and was taken at slightly different angles from each other in an overlapping series around the outcrop. The drone photos aimed to capture all the detailed geometry of the outcrop for precise DOM building.

Digital Outcrop Model Building

The images were processed to construct a 3D model using the Agisoft Metashape Professional

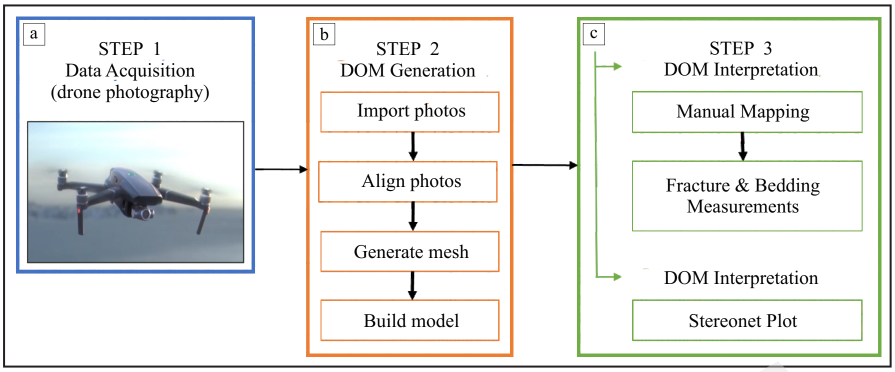

Figure 3. Basic workflow diagram showing the three main steps of the study: a). Step 1 - Data acquisition using a drone, b). Step 2 - DOM building in photogrammetry software, and c). Step 3 - Structural data extraction and analysis.

2.0.1 photogrammetry software. The photogrammetry processing steps from importing photos to the model building are shown in Figure 4. A total of 792,864 tie points in different dimensions were created from 1,880 aligned images. The point cloud was used to define the faces and shapes which form the depth map and mesh. Finally, the texture was constructed to give colour and detail to the 3D model when applied to the mesh by the mosaic blending model.

The DOM construction relied on direct georeferencing provided by a multi-constellation GNSS sensor and an Inertial Measurement Unit (IMU) onboard the aircraft. GNSS data indicated favourable Dilution of Precision (DOP) values consistently below 2, with a well-distributed

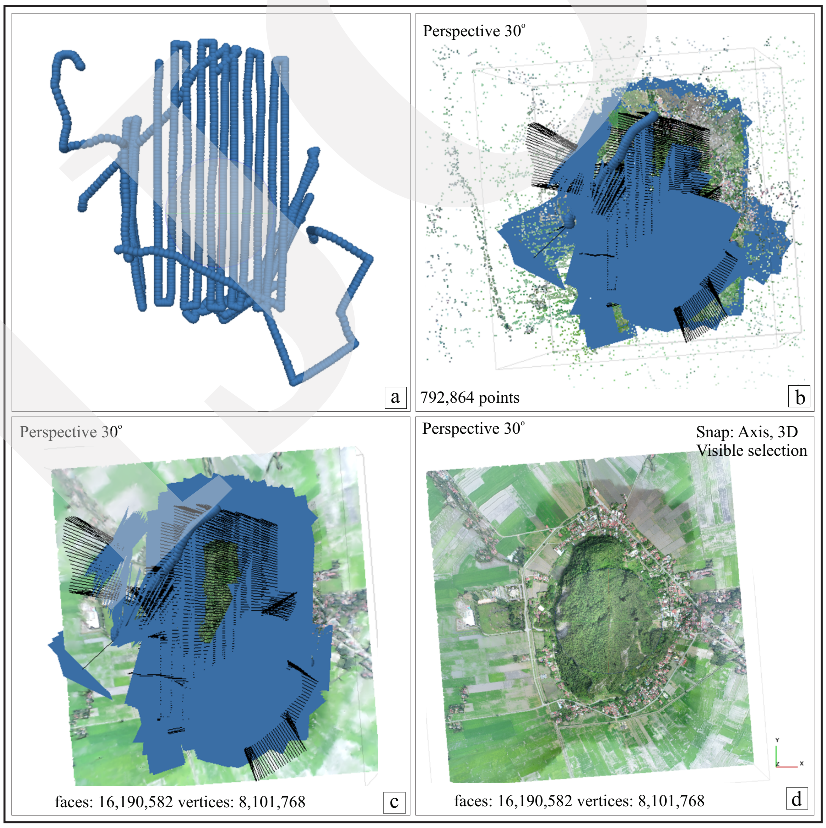

Figure 4. DOM photogrammetry processing steps. The workflow in sequential order: a) Import outcrop aerial photos, b) Alignment of mutual points in photos points and estimating photo locations, c) Depth map and mesh building, d) Texture atlas parameterization, blend textures, and tiled model building.

skyplot of satellites during the acquisition. The multi-constellation GNSS sensor minimized geometric uncertainties, ensuring that any potential distortions were within acceptable ranges. This direct georeferencing process is assumed to effectively rectify and correct geometric distortions in the images, thereby enhancing the accuracy of the 3D model to a degree that is sufficient for the study purposes, though it does not achieve millimeter-level precision.

Interpretation and Analysis Using DOM

Structural Analysis

The DOM was analyzed using the Lidar Interpretation and Manipulation Environment (LIME) software, developed by the Virtual Outcrop Geology Group (Figure 5). LIME supports 3D visualization of outcrop models and facilitates bedding and fracture mapping, along with digital measurements. The software provides a 3D DOM in orthographic projection mode, enabling accurate virtual orthorectification from any geological perspective. This process involves rotating the model to achieve an optimal viewing orientation and projecting all DOM points onto a plane perpendicular to the view direction. Integrated interpretation tools within LIME allow for precise measurement of distances and orientations, creation of lines and planes, and placement of points of interest. Structural features were manually mapped by selecting the intersection points of these features with the 3D model surface. Planar regression was used to determine the best-fit planes for bedding and fracture planes, minimizing the orthogonal distance between the 3D points and the plane to optimize the fit. LIME calculates and displays the plane orientation and scalar error and automatically records the orientation, position, length, and down-dip height of the planes. To ensure the reliability of the extracted structural data, several validation steps were implemented *i.e.* manual visual verification by the interpreter, multiple extractions to assess consistency, and comparison with field data. These measurements were designed to address uncertainty and confirm the accuracy of the extracted structures. The

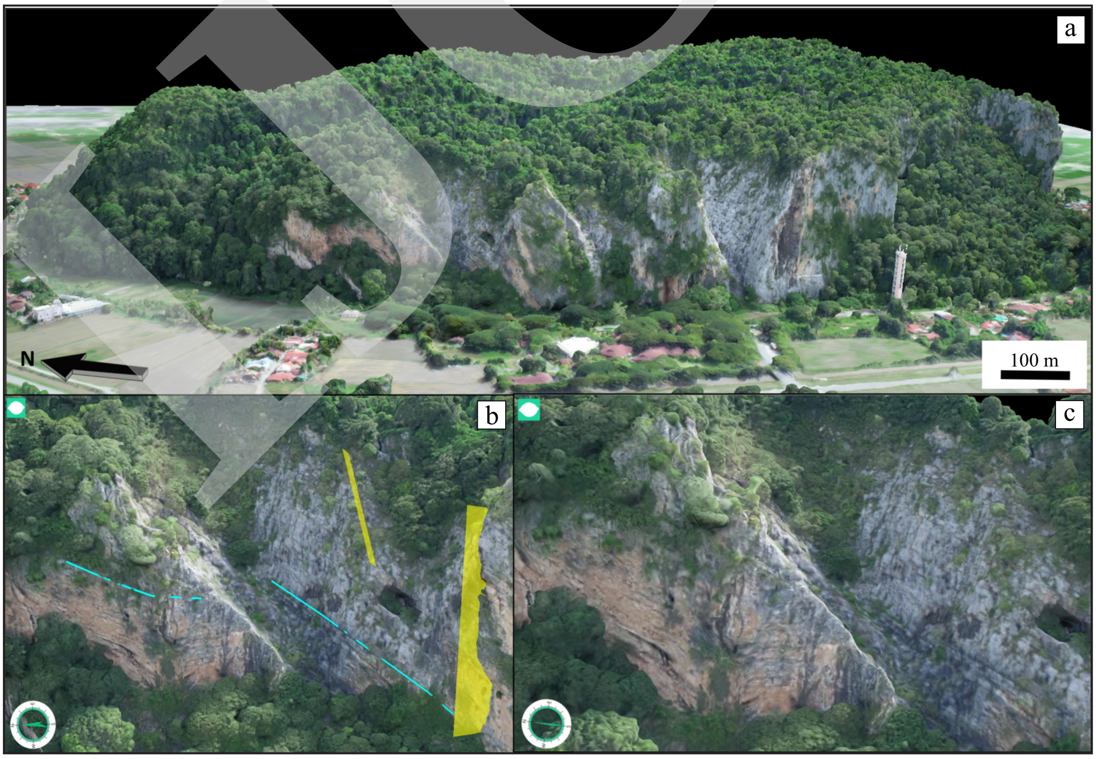

Figure 5. 3D DOM of Gunung Keriang. (a) Model visualisation in LIME software. (b) Lines (cyan blue) and fracture planes (yellow) interpretation in the graphical interface of LIME software. (c) The smoothened DOM with medium-quality resolution.

validated data were then plotted using Stereonet software (Allmendinger, 2013) version 11.5.1 for illustration and further analysis.

Analysis of Sinkhole

Visible sinkholes in the DOM were mapped, and their geometry information was extracted in the LIME software. Interpreted lines can be closed to form a polygon outline for sinkhole geometry and area measurement. The shape of the sinkhole (Figure 6) was defined by calculating the elongation ratio (R) between lengths of the maximum (MA) and minimum (mA) axes on plan view; the shape is described as circular when R equals 1 and increasing the value of R results in an elliptical ($1.21 < R < 1.65$) to elongated ($R > 1.8$) shape (Basso *et al*., 2013). The maximum axis is the line connecting the two most distant points of the sinkhole perimeter, whereas the minimum axis is the longest line on the perimeter that is perpendicular to the maximum axis.

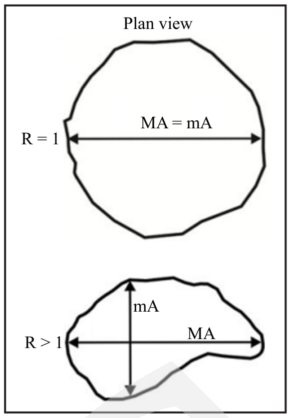

Figure 6. Plan view sketch of a sinkhole showing the shape definition parameters (Basso *et al*., 2013).

RESULTS AND DISCUSSION

The following part focuses on the extraction and interpretation of structural elements (bedding and fracture) and sinkholes on the DOM. The extracted data are compared with and validated against field data from Gunung Keriang, as reported in previous study by Aznan *et al*. (2024).

Structural Analysis: Bedding Planes

Analysis of bedding orientations on visible, exposed rock sections at the western and eastern flanks of the DOM was carried out. Notably, slumps and rock layers were easily identified on the DOM (Figure 7). The orientation of twelve bedding planes was measured and recorded (Table 1). The rocks are formed by gently dipping beds that strike in the NE-SW direction (average plane: 054°/31°) on the western flank, and are oriented in

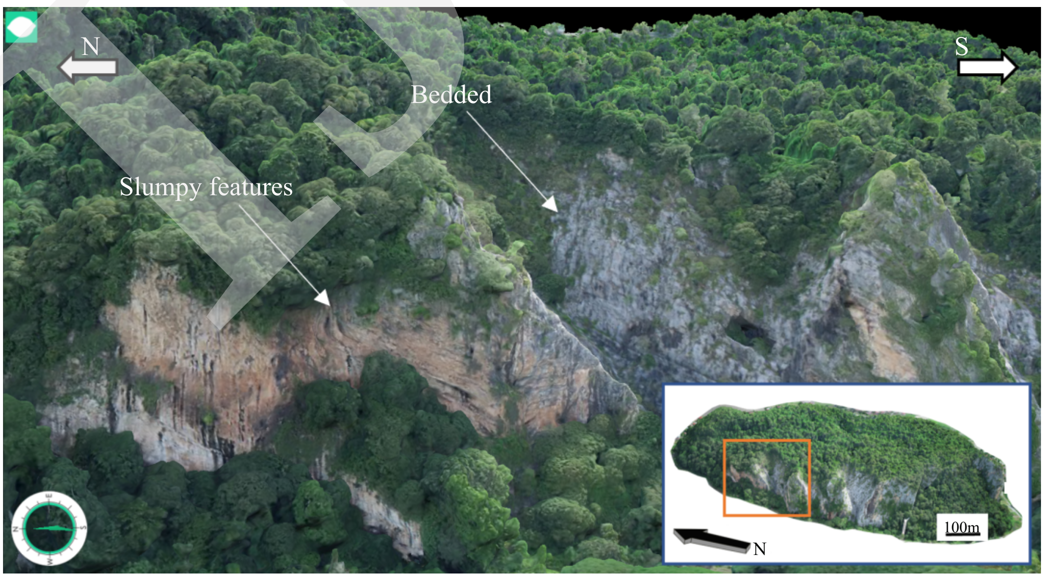

Figure 7. Sedimentary features observed on the Gunung Keriang DOM. The sedimentary features are well-bedded on the western flank with some slump features.

the NW-SE direction (average plane: 125°/27°) at the eastern cliff (Figure 8). The bedding orientations in the current spatial distribution form an upright, synclinal fold with a fold axis of 187°/24°, and an axial plane of 185°/86°. The folding suggests that there has been a shortening in the east-west direction.

The data extracted from the DOM (Figures 8a, c, and d) were compared with in-situ observations from strategically selected accessible areas (Figures 8e and 8f). The results confirmed that both the bedding orientations and measurements were consistent with expectations and within an acceptable range (Table 1).

Table 1. Summary of Bedding Plane Information Extracted from the DOM of the Western and Eastern Flanks of Gunung Keriang, as well as from In-situ Field Observations

Beddings	Western flank		Eastern flank	
	DOM	In-Situ	DOM	In-Situ
Number of readings	6		6	
Strike	45 - 75°	42°	110 - 140°	135 - 160°
Dip	20 - 45°	30°	16 - 37°	20 - 35°
Average Bedding Plane (Deduced from stereonet)	054/31		125/27	

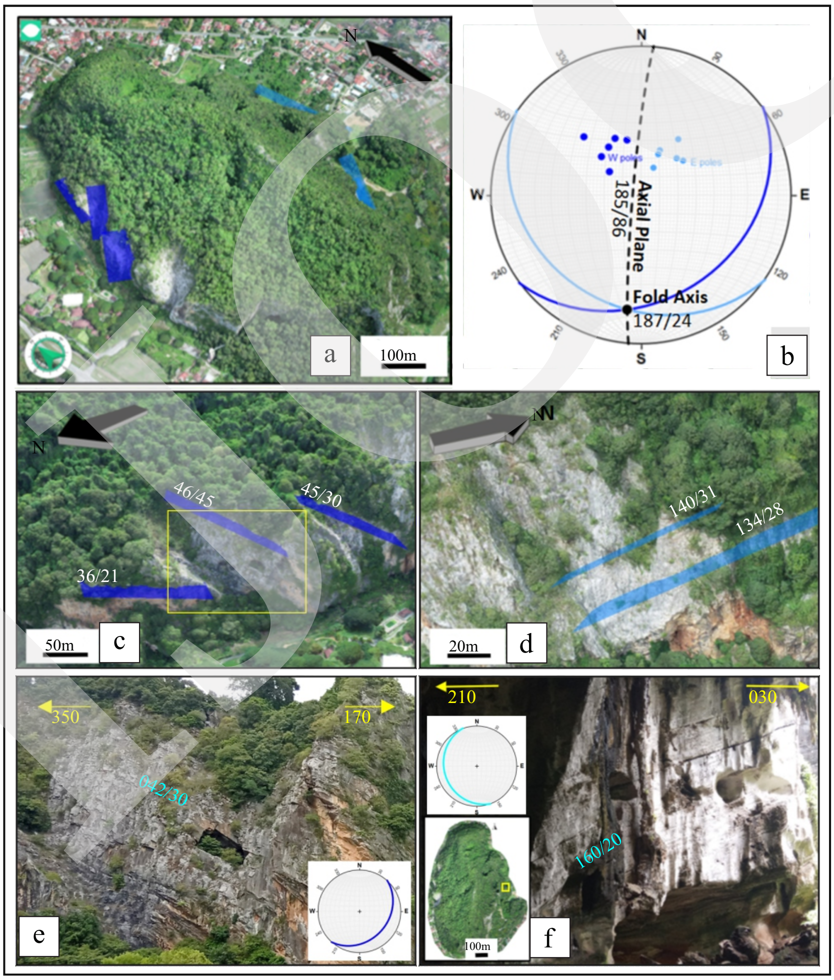

Figure 8. a. Bedding planes (dark blue and light blue coloured planes) interpreted on Gunung Keriang DOM. (b). The extracted bedding readings were plotted in stereonet to deduce its fold axis and axial plane of fold. (c). Three bedding planes (045°/30°, 046°/45°, 036°/21°) were traced at the western flank and; (d). Two bedding planes (140°/31°, 134°/28°) were traced at eastern flank of Gunung Keriang. (e) Outcrop view of the western flank shows well-bedded limestone with gentle dipping (bed orientation: 042°/30°) based on in-situ field measurements. (f) Gently-dipping limestone (bed orientation: 160°/20°) at Gua Terus on the eastern flank of Gunung Keriang, as observed from in-situ field data. The orientation of the bed is similar to the readings extracted from the DOM.

Structural Analysis: Fractures

In the fracture analysis, the surface expression of the DOM was used to delineate the fracture planes. A total of fourty-seven fractures were identified and measured on the Gunung Keriang DOM (Figure 9). The identified fractures can be subdivided into four fracture sets based on their dominant strike directions: NW-SE set, NE-SW set, N-S set, and E-W set (Table 2). The fracture analysis revealed that all the fracture sets are steep to nearly vertical dipping.

NW-SE Fracture Set

Eleven NW-SE fractures were extracted from the DOM. The NW-SE set has an average fracture plane of 128°/75° (Figure 10). Their fracture lengths range from 33 to 268 m, with an average length of 173 m. The mapped fracture planes have a down-dip height of 68 - 173 m. Field observations confirmed the presence of these fracture sets on all exposed sides of the outcrop, including the eastern flank, western flank (Figure 10b), and the southern area.

NE-SW Fracture Set

A total of nineteen NE-SW fractures were extracted from DOM. The average plane of the NE-SW set is 059°/61° (Figure 11). The fracture lengths range from 23 to 287 m, averaging 157 m. The down-dip height of the NE-SW fracture set is

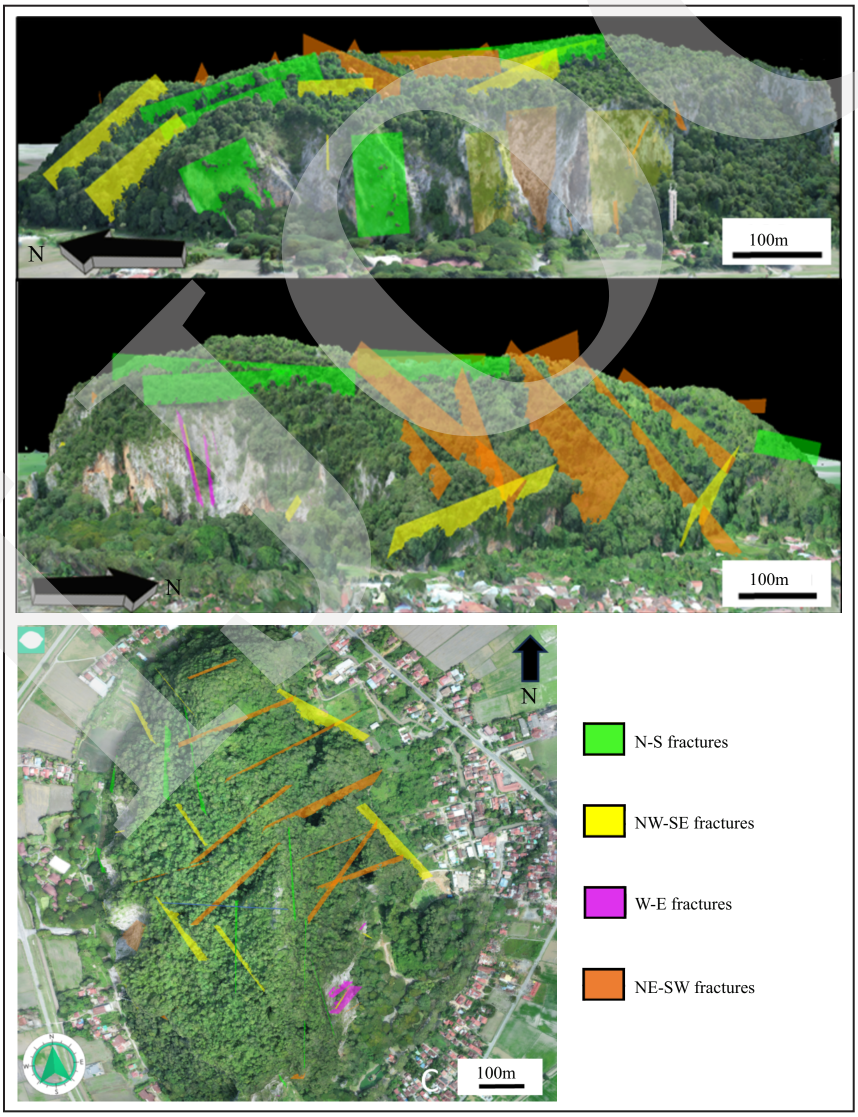

Figure 9. Four fracture sets identified in the Gunung Keriang DOM. (a) Western flank. (b). Eastern flank. (c) Top view.

Table 2. Fracture Data of Gunung Keriang

Fractures	NW-SE	NE-SW	N-S	E-W
Number of readings	11	19	12	5
Strike range (left-hand rule)	115-160°; 290-340°	053-075°; 205-250°	340°-000; 168-188°	081- 090°
Dip range	60-88°	60-89°	72- 9°	68-76°
Length range (m)	33-268	23-287	75 -17	31-196
Average length (m)	173	157	163	114
Down-dip height range (m)	68-173	24-175	89-168	40-116

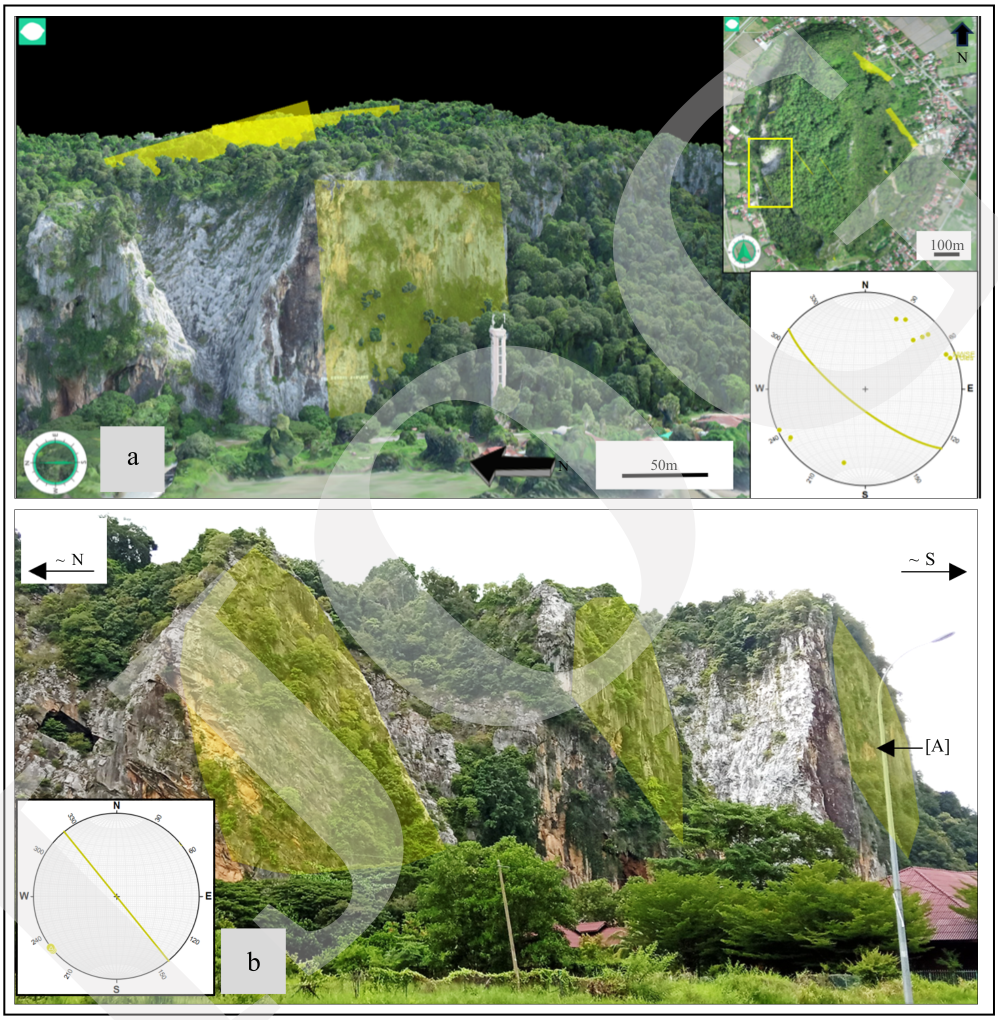

Figure 10. (a) NW-SE fractures (yellow surfaces) marked at the western flank of the DOM. The yellow box in the inset map shows the location of this view. The stereonet shows the poles of fractures and average plane orientation of NW-SE fractures (128°/75°). (b). NW-SE fractures at the in-situ western flank outcrop form major cliff faces, with an average plane orientation of 140°/90°. The NW-SE fracture at the southern end (marked by an arrow) corresponds to the same fracture location shown in (a).

24 - 175 m. This fracture set was mostly delineated at the middle part of the DOM. The NE-SW fractures are oriented parallel to the elongated direction of the sinkholes observed in Gunung Keriang. More details are elaborated in Karst Sinkhole and Cave Section. Additionally, similar trending fractures are observed on the western flank of the in-situ outcrop (Figure 11c), confirming their presence and consistency.

N-S Fracture Set

There are twelve N-S fractures that were traced in DOM. The average plane of N-S frac-

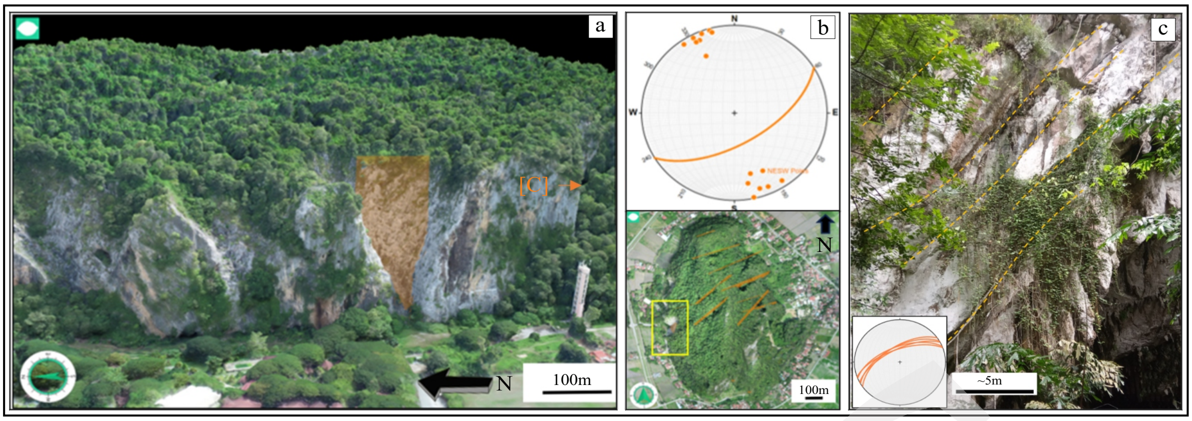

Figure 11. (a) One of the NE-SW fractures at the western flank of Gunung Keriang. (b) The yellow box in the map shows the location of the view shown in (a). The Stereonet displays the poles of these fractures and the average plane orientation of NE-SW fractures (059/61). (c) Fractures observed in the field near the cave entrance at the southern end (highlighted with an arrow in (a) exhibit the same NE-SW trend.

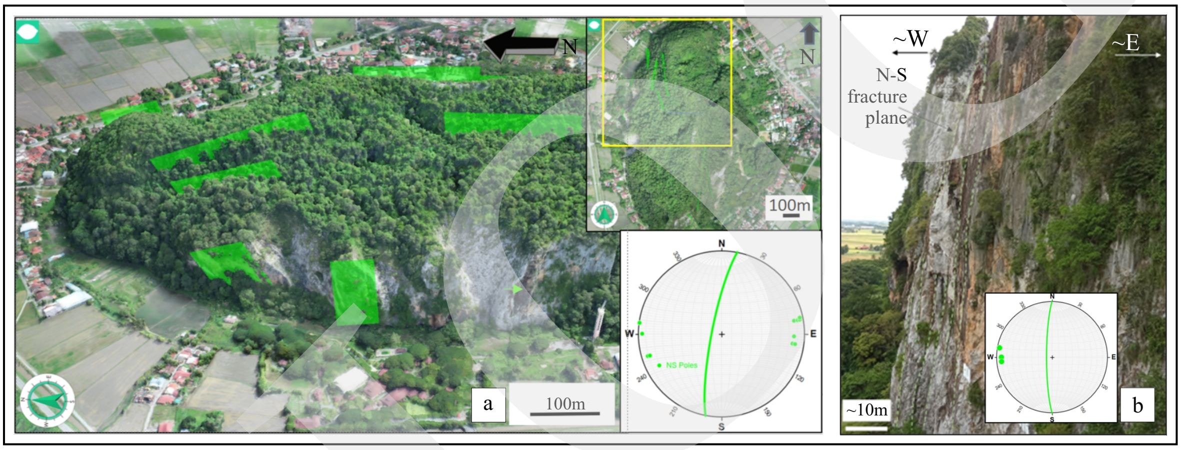

Figure 12. (a) N-S fractures (green surface) marked at the northern part of Gunung Keriang. The yellow box in the inset map shows the location of the view. The stereonet shows the poles of these fractures and the average plane orientation of the N-S fractures (191°/81°). (b) Detailed view of the N-S fractures observed at the western flank outcrop (highlighted with an arrow in (a). The in-situ measured average plane orientation of these fractures is 185°/81°.

tures is 191°/81°. (Figure 12). The fracture lengths range from 75 - 317 m, with an average length of 163 m. The down-dip height of the fracture set is 89 - 168 m. This set mainly occurred at the northern end of the Gunung Keriang. These prominent fractures were also observed at both the eastern and western sides of the limestone hill, confirming the presence and consistency of the fracture set (Figure 12b).

E-W Fracture Set

E-W fractures were primarily visible at the eastern flank of the DOM. A total of five E-W readings were mapped. These fractures have an average plane of 085°/72° (Figure 13). The lengths of E-W fractures range from 31 - 196 m and the average was 114 m. The down-dip height of the fracture set is 40 - 116 m. In addition to these observations, in-situ field data revealed a minor E-W fracture set which cross-cuts the thick limestone beds at the western and eastern flank (Figure 13b) outcrops, providing further validation of the E-W fractures.

Karst Sinkhole and Cave

Two types of karst features, sinkholes, and caves were identified on the Gunung Keriang DOM (Figure 14). In the DOM, five sinkholes (named J, K, L, M, N) were mapped with coverage areas ranging from 1770 to 2950 m^2 (Table

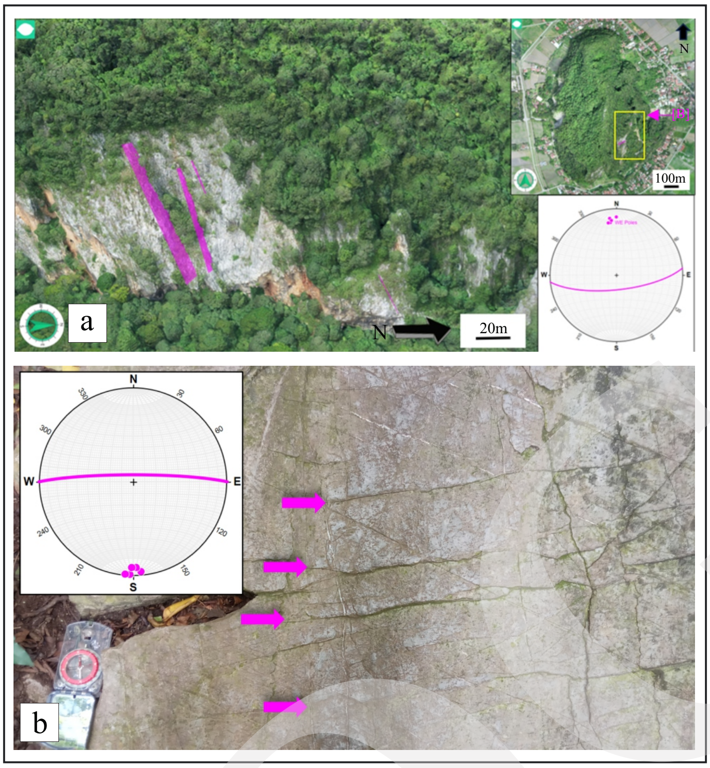

Figure 13. (a) E-W fractures (magenta surfaces) marked at the eastern flank of Gunung Keriang DOM. The yellow box in the inset map shows the location of the view. Stereonet shows the poles of fractures and average plane of E-W fractures (085°/72°). (b) Hiking trail at the eastern flank of Gunung Keriang showing the dense occurrences of E-W fractures, as marked by arrows.

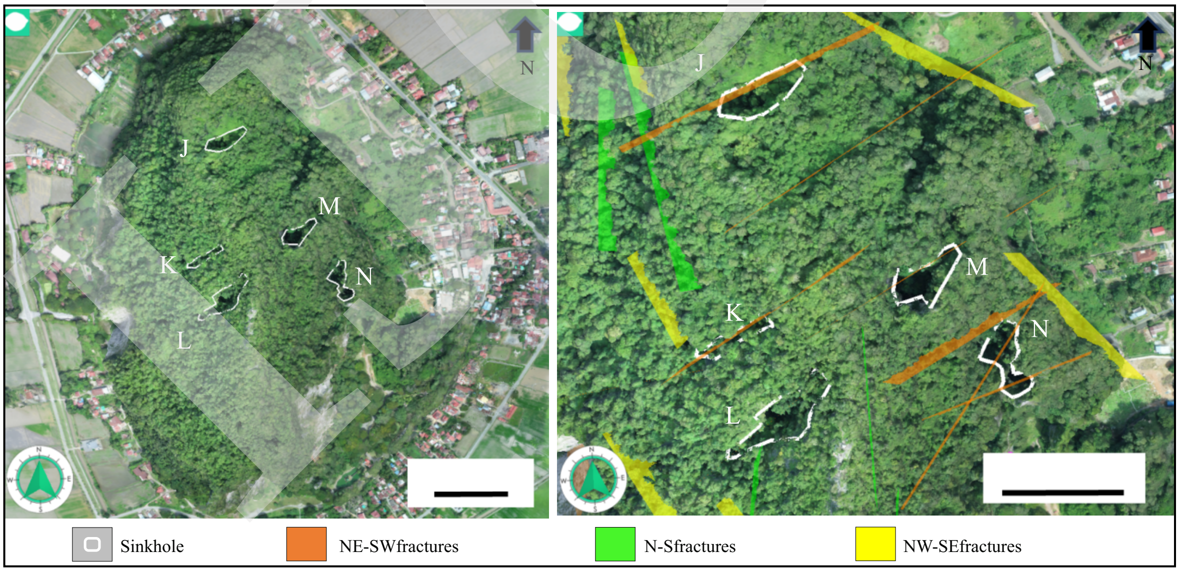

Figure 14. (a) Five sinkholes ("J", "K", “L”, “M”, “N”) were traced at the top of Gunung Keriang DOM. (b) Sinkholes “J”, “K”, “L”, “M” are parallel to the NE–SW fractures (orange).

3). The sinkhole maximum axis lengths (MA) are 83 - 161 m, with an azimuth of 060° -065°, except for one reading in 350°. In general, the sinkholes have an elongated shape and are parallel to the NE -SW fracture set, except for sinkhole "N" which has its maximum axis oriented in the N -S direction. The shape of sinkhole "N" is wider at its ends and narrow in the middle.

Table 3. Geometry Information of Sinkholes Extracted from DOM

Sinkhole	Area (m^2)	Maximum axis length, MA (m)	Maximum axis azimuth	Minimum axis length, mA (m)	Elongation ratio, R=MA/mA	Shape
J	1950	93	N 065	41	2.3	Elongated
K	1770	121	N 065	19	6.4	Elongated
L	2950	161	N 060	47	3.4	Elongated
M	2715	83	N 060	52	1.6	Elliptical
N	2830	91	N 350	44	2.1	Elongated

This could indicate a compound sinkhole where two sinkholes merged when the rocks in between them collapsed.

Gua Terus cave is a larger-scale karstification feature formed in the body of the Gunung Keriang limestone hill (Figure 15). The cave has two entrances on the eastern hill and SW flanks. This 600 m long cave cuts through the limestone hill in an ~NE -SW direction. The cave entrances are located approximately 100 m above the ground. However, the cave geometry was not directly visible on the DOM, and the shape or path was extracted from the official information board of Gunung Keriang. The strong alignment of NE -SW fractures, sinkhole elongation, and cave directions suggest that karst formation is likely controlled by the NE -SW fracture set.

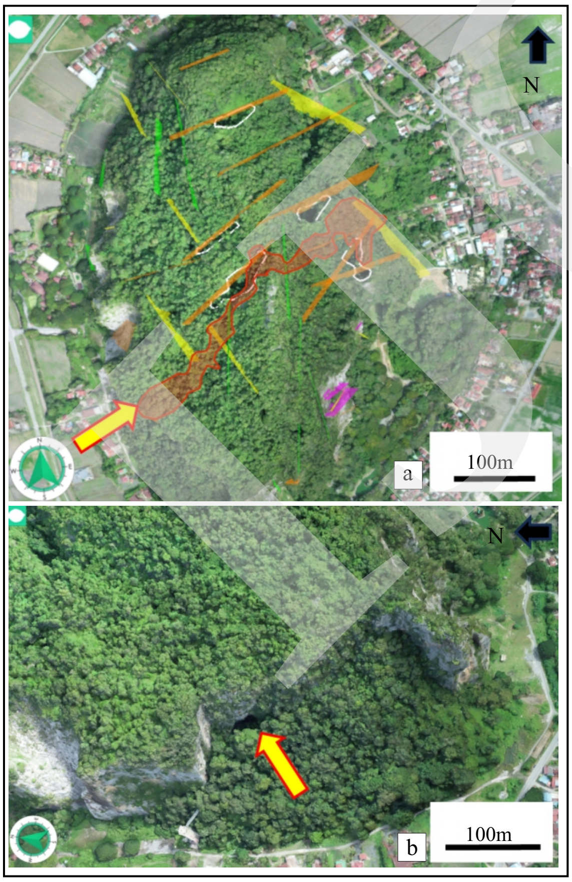

Figure 15. (a) The 600 m path of Gua Terus (highlighted in red) connects the eastern flank (recreation park) to the SW flank of the hill. The arrow marks the SW cave entrance of Gua Terus. (b) Zoomed-in view of SW cave entrance.

Synthesis and Discussion

Structural Geology and Karst

Structural analysis was conducted on beddings and fractures of the Gunung Keriang DOM. The limestone beds are characterized by gently inclined planes with NE -SW and NW -SE strikes. The beds formed an upright synclinal fold and gently plunged at 24° toward the south (Figure 16).

A total of four fracture sets (striking in NW -SE, NE -SW, N -S, and E -W directions) were sampled on the DOM. All fractures are dipping steeply. The NW -SE and NE -SW fracture sets can form a conjugate pattern, and may indicate an E -W shortening. It also corresponds to the N -S fold of Gunung Keriang, which can form under the same activity. The N -S fracture set is parallel to the fold axis, and may be considered strike fractures.

The highly fractured outcrop may have led to the development of the limestone medium to large scale karst features. Generally, the karst is well-developed in the NE -SW direction, which is controlled by the corresponding fracture set (Figure 16). These fractures acted as the main fissure contributing to the dissolution of the limestone and existing cavities.

DOM Application in Geological Study

This paper introduces the drone-based photogrammetry technique to produce a digital

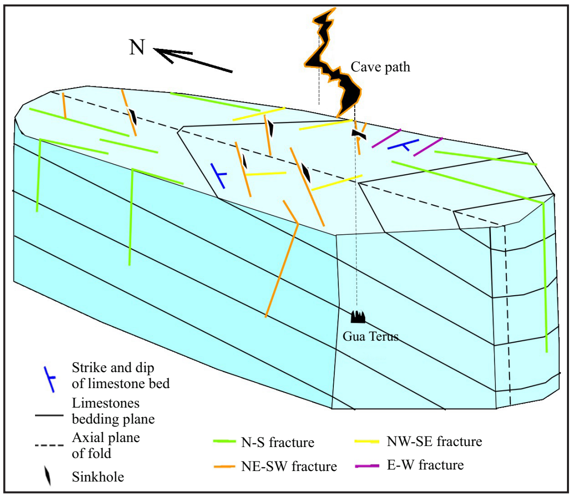

Figure 16. Schematic geological model of Gunung Keriang based on DOM interpretation and analysis.

outcrop model (DOM) that is particularly useful for structural analysis of challenging outcrops. The analysis of the DOM demonstrates that the data collected complements traditional field measurements. Additionally, the DOM allows for the extraction of information from partially inaccessible outcrops. Traditional structural measurements were often taken from a distance in high-elevation areas that were difficult to access, but the DOM enables more representative measurements to be analyzed with greater accuracy and safety. Despite some discrepancies and the lack of millimeter-level accuracy, the DOM provides a solid foundation for general structural studies. For more detailed mapping requirements, however, Real-Time Kinematic (RTK) or post-processing positioning enhancements would be necessary.

Conclusions

This work presents the development of a digital outcrop model (DOM) of the Permo-Triassic limestone of Gunung Keriang in NW Peninsular Malaysia to provide a structural analysis of fracture and karst features. Due to the thick vegetation in Gunung Keriang, limited localities were physically accessible, and some of the observations/measurements were conducted from a distance. From the DOM analysis, the bedding, fractures, and karst features of Gunung Keriang could be extracted, measured, and then calculated with high precision, which complements the field observations and measurements. The overall bedding orientation of this limestone hill reveals an upright NS trending synclinal fold with a gentle plunge of 24° toward the south. A total of four fracture sets (NW -SE, NE -SW, N -S, and E -W striking) were identified in the DOM, and are generally dipping steeply. The NW -SE and NE -SW fracture sets displayed a conjugate pattern compatible with an E -W shortening deduced from the fold orientation. The N -S fracture set is thought to be the strike fractures in the fold. Karst features such as caves and sinkholes commonly occur in Gunung Keriang. Five sinkholes were detected in the DOM, and their shapes are mostly elongated in the NE -SW direction, parallel to the cave path of Gua Terus. The NE -SW-oriented karst features of Gunung Keriang are believed to be controlled by fracture sets of the same direction.

Acknowledgements

This work is funded by The Yayasan Universiti Teknologi PETRONAS (YUTP) (0153LC-307) Project, which is supported by The Institute of Hydrocarbon Recovery (IHR), UTP. Many thanks to the developers of Agisoft Metashape (trial), LIME (academic license), and Stereonet 11 for creating the software that aided this study.

References

Allmendinger, R., 2023. *Stereonet (Version 11.5.1)*. Available online at https://www.rickallmendinger.net/stereonet, check on 10/30/2023. Google scholar.4.

Aznan, M.A., Mansor, N.A., Choong, C.M., Abdu Rahman, S.S., Md. Yusof, M.A., and Mohamed, M.A., 2024. Fracture Model and Structural History of Gunung Keriang, Kedah.

Bulletin of the Geological Society of Malaysia, 77, p.37-46. DOI: 10.7186/bgsm77202405.

Basso, A., Bruno, E., Parise, M., and Pepe, M., 2013. Morphometric analysis of sinkholes in a karst coastal area of southern Apulia (Italy). *Environmental Earth Science,* 70, p.2545-2559. DOI: 10.1007/s12665-013-2297-z.

Buckley, S.J., 2019. LIME: Software for 3-D Visualization, Interpretation, and Communication of Virtual Geoscience Models. *Geosphere,* 15 (1), p.222-235. DOI: 10.1130/GES02002.1.

Buckley, S.J., Howell, J.A., Naumann, N., Lewis, C., Chmielewska, M., Ringdal, K., Vanbiervliet, J., Tong, B., Mulelid-Tymes, O.S., Foster, D., Maxwell, G., and Pugsley, J., 2022. V3Geo: A Cloud-based Repository for Virtual 3D Models in Geoscience. *Geoscientific Communication,* 5, p.67-82. DOI: 10.5194/gc-5-67-2022.

Cardozo, N. and Allmendinger, R.W., 2013. Spherical projections with OSXStereonet. *Computers and Geosciences,* 51, p.193-205. DOI: 10.1016/j.cageo.2012.07.021.

de Coo, J.M.C. and Smith, O.E., 1975. The Triassic Kodiang Limestone Formation in Kedah, west Malaysia. *Geologie en Mijnbouw,* 54 (3/4), p.169-176.

Foo, K.Y., 1983. The Palaeozoic sedimentary rocks of Peninsular Malaysia - Stratigraphy and correlation. *Proceedings of the Workshop on Stratigraphic Correlation of Thailand and Malaysia*, p.1-19.

Gobbett, D.J. and Hutchison, C.S., 1973. *Geology of the Malay Peninsula (West Malaysia and Singapore)*. John Wiley & Sons, Inc.

Ishii, K.S. and Nogami, Y., 1966. Ordovician and Silurian conodonts from Langkawi Islands. *Geology of Paleontology of Southeast Asia,* 3, p.1-29.

Kobayashi, T. and Tamura, M., 1968. Myophoria (s.l.) in Malaya in a Note on the Triassic Trigoniacea. *Geology of Paleontology of Southeast Asia*, Univ. of Tokyo Press.

Meor, H.H., 2013. Post-Conference Field Excursion to Northwest Peninsular Malaysia. *Third International Conference on Palaeontology of South East Asia 2013*.

Metcalfe, I., 1981. Permian and Early Triassic conodonts from Northwest Peninsular Malaysia. *Geological Society of Malaysia Bulletin,* 14, p.119-126. DOI: 10.7186/bgsm14198106.

Metcalfe, I., 2009. *Stratigraphic and tectonic implications of Triassic conodonts from northwest Peninsular Malaysia*. Cambridge University Press, 127 (6), p.567-578. DOI: 10.1017/S0016756800015454.

Metcalfe, I., 2011. Palaeozoic-Mesozoic history of SE Asia, *In*: Hall, R., Cottam, M.A., and Wilson, M.E.J., (eds.) *The SE Asian Gateway: History and Tectonics of the Australia-Asia Collision. London.* Geological Society, *Special Publications,* 355, p.7-35. DOI: 10.1144/SP355.2.

Senger, K., Betlem, P., Grundvåg, S.-A., Horota, R. K., Buckley, S.J., Smyrak-Sikora, A., Jochmann, M.M., Birchall, T., Janocha, J., Ogata, K., Kuckero, L., Johannessen, R.M., Lecomte, I., Cohen, S.M., and Olaussen, S., 2021. Teaching with digital geology in the high Arctic: opportunities and challenges, *Geoscientific Communication,* 4, p.399-420. DOI: 10.5194/gc-4-399-2021.

Tavani, S., Corradetti, A., Mercuri, M., and Daniel Seers, T., 2024. Virtual Outcrop Models of Geological Structures, From the Construction of Photogrammetric 3D Models to Their Application Towards the Analysis of Geological Structures. *Società Geologica Italiana.* DOI: 10.3301/MON.2024.01.

Yusof, M.A.M., Choong, C.M., Mohamed, M.A., Abdu Rahman, S.A., Aznan, M.A., and Mansor, N.A., 2022. Natural Fracture System of Gunung Keriang, Kedah: *GEOSEA XVII*, Bayview Hotel, Langkawi, Malaysia. 17-21 Oct 2022.